Proceedings of the SEM Annual Conference
June 7-10, 2010 Indianapolis, Indiana USA

Loading Rate Effect on Tensile Failure Behavior of Gelatins under Mode I

Paul Moy
(pmoy@arl.army.mil)

Mark Foster
(mark.foster12@us.army.mil)

C. Allan Gunnarsson
(allan.gunnarsson@us.army.mil)

Tusit Weerasooriya
tusitw@arl.army.mil

Army Research Laboratory
Weapons and Materials Research Directorate
Bldg 4600 Deer Creek Loop
Aberdeen Proving Ground, MD 21005-5069

ABSTRACT

For decades, ballistic gelatin has been used as a tissue surrogate to test and evaluate bullets and firearms due to its similar viscosity to natural tissue. However, the high water content in ballistic gelatin makes it unstable at room temperature, and therefore causes it to have a poor shelf life. The development of polymer-based gels has shown promise as an alternative tissue surrogate. Polymer gels such as Perma-Gel are stable at room temperature and can be stored for long periods of time. Gels often fail due to tensile stresses during penetration. The failure behavior in tension is highly influenced by the presence of defects, such as cracks and voids, in the bulk material. A mode I experimental method was developed to obtain tensile failure criteria for the initiation and propagation behavior of these types of soft materials. Digital image correlation is used to determine the full-field surface strains around the crack tip to obtain a quantitative measure of the critical strain-field required for initiation and propagation of failure due to a defect. This systematic study utilizes these experimental techniques to determine the critical criteria for crack growth initiation and crack propagation of ballistic gelatins and a polymer gel as a function of loading rate. This paper presents experimental methodologies and results from Mode I fracture experiments including measured critical energy and strain-based criteria for failure initiation and growth, as well as their dependence on the rate of loading.

INTRODUCTION

For decades, the tissue surrogate ballistic gelatin has been used as a standard target to test and evaluate bullets and firearms [1]. This material has the approximate density and viscosity of biological tissues and thus provides an excellent substitute for biological subjects. Typically, ballistic gelatin of a certain mixture and size is shot with a firearm from a standard distance. The bullet would lodge within the gelatin and the depth of penetration would be measured to determine the approximate effect of the projectile on tissue. Other ballistic studies on gelatins have involved the use of high speed imaging to examine the temporary and permanent cavities inflicted by the penetration of the bullet [2-4]. The study of the formation of these cavities in ballistic gelatin was typically a qualitative investigation rather than a quantitative one. Nevertheless, these efforts offered an insight into the effectiveness of the bullet or weapon.

T. Proulx (ed.), *Dynamic Behavior of Materials, Volume 1*, Conference Proceedings of the Society for Experimental Mechanics Series,
DOI 10.1007/978-1-4419-8228-5_4, © The Society for Experimental Mechanics, Inc. 2011

Ballistic gelatin is produced from a mixture of protein-based powder and water; this causes it to degrade over time and thus having a short shelf life. It has been noted that the mechanical properties of ballistic gelatin will begin to change in as short of a time as 1-2 days, or even shorter if left out at room temperature and exposed to dehydration due to evaporation. Recently, polymer based gels, such as Perma-Gel™ has been introduced to the market as an alternative to ballistic gelatin. According to the manufacturer of Perma-Gel (Perma-Gel, Inc., Albany, OR), the material is 100% synthetic, clear, and reusable. Also, the manufacturer maintains that this polymer gel is closely matched in physical and mechanical properties to 10% ballistic gelatin. It differs significantly from 20% ballistic gelatin, which is another tissue surrogate used by NATO [5]. An advantage of polymer based gels is the ability to tailor them to potentially simulate the physical and mechanical properties of actual tissues and organs. This is not possible with ballistic gelatin due to its inherent homogeneity and fixed mechanical properties, which is unlike most biological tissues.

Tissue simulants provide valuable information about penetration and wound mechanics; therefore, when gelatins are used as tissue simulants, it is necessary to fully understand the mechanical responses of them under these impact conditions to obtain material models for different stress states. During these impact and penetration events, these tissue simulants fail most frequently due to tensile stresses at high loading rates, causing a pre-existing defect to grow. Therefore, it is essential to obtain the constitutive and failure behavior of these gelatins under tensile loading conditions up to high loading rates, as well as other stress states.

Gelatin like material has been characterized for mechanical responses using several different techniques. Moy et al [6] conducted uniaxial compression of 20% ballistic gelatin as well as physically associating gels at intermediate and high strain rates. Their high strain rate experiments were performed using aluminum Split-Hopkinson Pressure Bars under dynamic stress equilibrium. Similarly, Salisbury et al [7] characterized ballistic gelatin under compression at different loading rates including high rates using a polymeric Hopkinson bar apparatus. Juliano et al investigated multiple mechanical characterization methods of biomimetic gels and explained the modulus relationship between these techniques [8].

There are only few studies on the tensile behavior of soft materials, such as tissue simulants, due to a lack of good experimental methods including gripping techniques. Additionally, there are even fewer studies in literature on fracture behavior of soft materials due to the difficulty in measurement of strain and displacement fields around the crack-tip. Previously, the authors developed experimental methods to obtain the tensile behavior of 20% ballistic gelatin under different strain rates up to 1/s [9]. Gelatins have similar characteristics to elastomers, which include a high stretch ratio. Zhang et al [10] investigated the resistance to Mode I fracture of natural rubber with crystallite fillers. They used a photo-elastic technique to determine the strain field at the notch-tip, and were able to study the fracture speeds as a function of elastic stored energy, thus obtaining the effect of crystallites on the fracture behavior. An experimental technique was developed by the authors previously to perform notched tensile fracture experiments on ballistic gelatin at low loading rate [11]. The work in this paper extends previous effort to obtain the fracture behavior for both 10% and 20% ballistic gelatin and the polymer gel commercially known as Perma-Gel, as a function of loading rate.

The major challenge associated with fracture experiments on ballistic gelatin is accurately measuring strain in the gage section of the specimen to obtain the strain distribution around the crack. Digital image correlation (DIC) technique was used to measure strain fields in the gage area and around the crack, similarly to the method used previously for tensile experiments [9] and fracture experiments [11]. DIC is a non-contact optical technique to measure surface displacements. Digital images are acquired during the test and, subsequently, the images are post processed with specialized software to convert pixel patterns into displacement/strains [12-16].

In the past several years, commercially available DIC systems have been extensively used to obtain axial and shear strains simultaneously. DIC systems can measure strain in complex states, and have the unique ability to acquire full-field strain measurements over a large area. Strain gages and extensometers are generally applicable for only one-dimensional strain measurements, and provide an average strain at a single point. Furthermore, strain gages and clip-on extensometers are not feasible for use on gelatin or other soft materials due to their susceptibility to damage the soft material. The sharp edges of an extensometer or metal foil gage would lead to premature failure at these locations during loading. The DIC technique allows better full-field measurement of displacement and deformation while eliminating any possible damage due to instrumentation.

MATERIAL

Both 10% and 20% (by mass) ballistic gelatin samples were made of 250 bloom type A ordnance gelatin (GELITA USA Inc., Sioux City, IA) with 40°C ultra-pure filtered water. The mixture was stirred slowly with a cake mixer to dissolve all the particles and to remove air bubbles. The solution was then poured into aluminum molds in the shape of the tensile specimen geometry. It is vital that the solution be poured into the molds in a very slow and deliberate manner to avoid frothing of the solution and formation of air bubbles in the gage length. Specimens with bubbles in or near the gage length are deemed unusable for experiments. The gelatin mixture begins to congeal gradually even at room temperature, at which the mold is then placed in a refrigerator. The ballistic gelatin specimens are prepared when the experiments are to be carried out the following day to ensure that the properties do not change. The specimens tend to dehydrate and thus the surfaces become hard when left at ambient room conditions. Therefore, individual ballistic gelatin specimens were removed from the molds just prior to testing.

Perma-Gel was acquired as a test block form about the size of a typical ballistic gelatin target (444 mm x 292 mm x 127 mm). To fabricate the Perma-Gel specimens, small pieces were extracted from the block and placed in an open-faced aluminum mold over a hot plate that was set to a temperature of about 120°C. The melting point for Perma-Gel is about 70°C. This procedure was repeated several times until the Perma-Gel filled the mold and matched the mold surface evenly.

MODE I FRACTURE EXPERIMENTS

Fracture experiments on gelatin were conducted using a tensile specimen that was inserted into the loading machine with special grips; a 1.75 mm deep pre-crack was created in the specimen just prior to testing. Since both the ballistic gelatin and Perma-Gel are so supple, the pre-crack was carefully initiated with a razor blade that was pressed across the edge of the gel specimen at the center of the gage length while it was in the grips. Notching after mounting the specimen into the grips ensured that no further crack growth was caused by handling the specimen. A custom designed jig was used to hold the razor blade and provide a fixed depth of the notch at the center of the sample; a backing piece was used to prevent the specimen from being “pushed” or bent by the razor.

The authors designed a “shoulder supported” tensile grip made from acrylic for the gelatin specimens. Schematic drawings of the specimen and grip fixture are shown in Figure 1. The dimensions in the drawing are displayed in inches. The gage length of the specimen is 25.4 mm, with a width (parallel to the crack) of 12.7 mm and a thickness of 9.5 mm. Also, the curvature of the shoulder was optimized to mitigate failure outside the gage section. Before settling with the shoulder curvature in the figure, several design iterations of the curvature were explored. It was determined that the radius of approximately 53.98 mm at the shoulder minimized the failure of the gelatin at the gage length/grip interface.

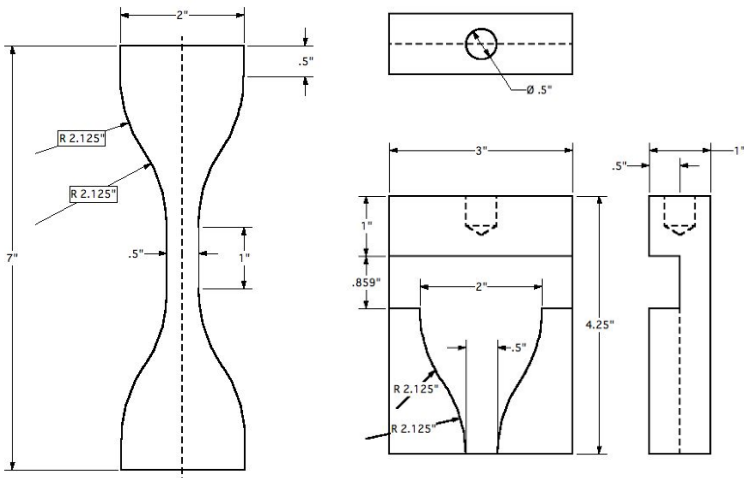

(a) (b)

Figure 1. Schematic Drawing of the Ballistic Gelatin (a) Specimen Geometry and (b) Tensile/Fracture Gripping Fixture

Prior to testing, the entire gage area of the specimen was speckled with a dark-colored ink using an airbrush for the digital image correlation measurements. Compared to the speckle pattern used for tensile experiments in the previous study [9], a much finer pattern was applied for these experiments. This finer speckles allowed measurement of the strain field around the crack tip at higher resolution during initiation and propagation of the crack compared to the previous study [11]. The measured load and displacement data were recorded and synchronized with the corresponding digital images taken during loading. The experiments were conducted at two different constant displacement rates: 0.127 mm/s (slow rate) and 127 mm/s (high rate). A single camera was configured to record images for 2D correlation, assuming minimum out-of-plane displacement during the experiment. Two different cameras were used for the two displacement rates. A Photron APX-RS camera, set to a frame rate of 1000 fps with resolution of 1024 by 1024, was used for the high rate experiments. The test images for the low rate experiments were recorded with a Point Grey Research camera at a frame rate of 4 fps and 1024 by 1024 resolution.

RESULTS AND DISCUSSION

Data obtained from a typical experiment are shown in Figures 2-7, in this case, for 20% ballistic gelatin at slow loading rate. Figure 2 shows the load-displacement plot from the fracture experiment for this gelatin with a series of corresponding correlated images at discrete times during the test. Each of the contour pictures represents the 2D strain field in the direction of loading and noted as e_{yy}. The color scale on the first four correlated images (0.13 to 0.23) is different from the scale on the last four images (0.1 to 0.4). The maximum e_{yy} value was extracted in the vicinity of the crack tip from the correlated images. The values are indicated below on each picture of the graph. There is a critical point at which the crack "pops" and begins to propagate across the specimen. This occurs 82.7 seconds after the test begins. Up until this point, the crack-tip-opening-displacement (CTOD) grows in the vertical direction, but the length of the crack remains constant. The maximum e_{yy} strain reaches a critical value of 0.18, when the pre-crack begins to propagate. The load at this point is 4.1 N, which is lower than the maximum load. The load increases beyond the critical point to a maximum of 4.7 N and then starts to decrease rapidly as the crack tip accelerates to failure. The maximum strain measured at the vicinity of the crack tip reaches 0.22 at the maximum load of 4.7 N. Subsequently, the maximum e_{yy} strain continues to increase after the peak load up to about 0.38 just before complete specimen failure.

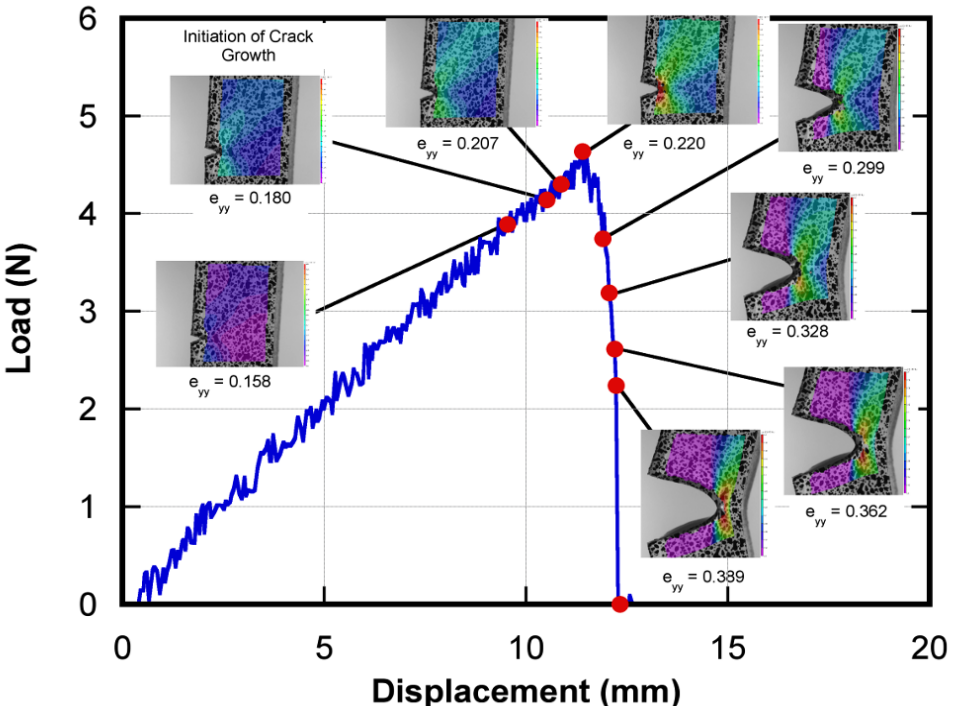

Figure 2. Load-Displacement for 20% Ballistic Gelatin Fracture Experiment at Low Rate with Measured Strain Fields in the Loading Direction Around the Crack-tip

Figure 3 displays the images that are embedded in Figure 2 with more detailed e_{yy} fields at corresponding times; time of zero ms corresponds to the beginning of loading. These pictures provide a close-up view of the strain field including the minimum and maximum values of the color contour scale. From these set of pictures, it can be seen that the strain field is symmetrically distributed along the crack tip during the entire experiment. The strain fields are entirely concentrated at the crack tip. The strain is nearly zero directly above and below the cracked surface in the ballistic gelatin.

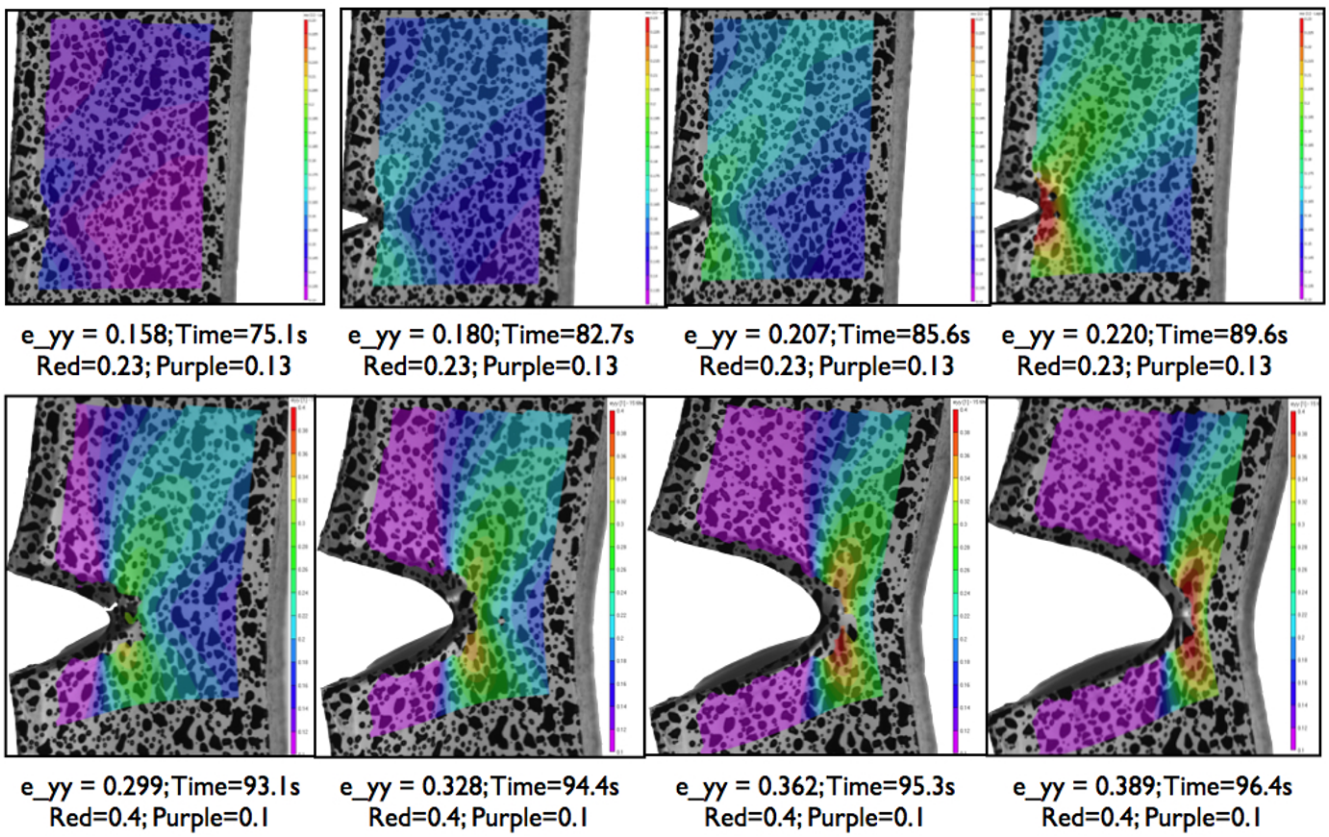

Figure 3. Strain-Field Around the Crack-Tip for 20% Ballistic Gelatin at Low Rate Showing Maximum Strain Values in the Loading Direction. Crack growth begins second picture, top row (82.7 seconds).

The maximum strain vs. time for 20% ballistic gelatin at slow rate is shown in Figure 4. The strain data is the maximum value obtained at the crack tip and is in the direction of loading. The figure also includes the corresponding load history of the experiment. The measured e_{yy} strain is constant up to the time at 82.7 seconds, which is when the crack begins to grow across the specimen. The black markers in all the figures indicate the point where the crack growth initiates. The load continues to increase at a constant rate for a period of time after crack initiation; it then starts to decrease rapidly as the specimen fails. The maximum strain, e_{yy}, increases approximately linearly at low rate until the load reaches the critical point. After this point, the rate of increase of e_{yy} is significantly higher compared to the initial rate before the critical load.

The crack length and load history plots for 20% ballistic gelatin at slow rate is shown in Figure 5. The crack length grows at a much higher rate after the critical point, which is indicated in the graph by the black markers. From the crack length measurements, the crack tip velocity was derived and is shown in Figure 6. Again, the crack tip velocity increases significantly after the critical crack initiation point. In both Figures 5 and 6, crack length and crack-tip velocity do not deviate significantly from their initial values until the load reaches the critical point.

Figure 7 shows the energy imparted to the 20% ballistic gelatin as a function of the measured crack velocity at slow rate. The energy is calculated by integrating the load vs. displacement curve. The displacement in this case is the relative displacement at the loading grips. The black marker indicates the critical energy (22.1 mJ) at the crack growth initiation point. Energy imparted to the specimen increases rapidly as the velocity of the crack-tip

increases. When the crack-tip velocity reaches around 1 mm/s, subsequent crack growth occurs at an approximate steady value of 29 mJ energy.

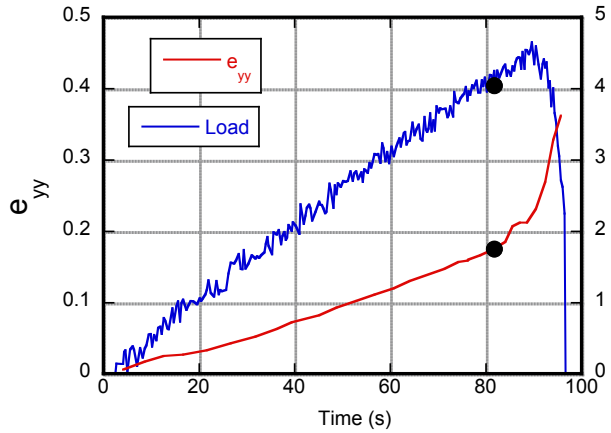

Figure 4. Maximum Strain and Load vs. Time for 20% Ballistic Gelatin at Low Rate

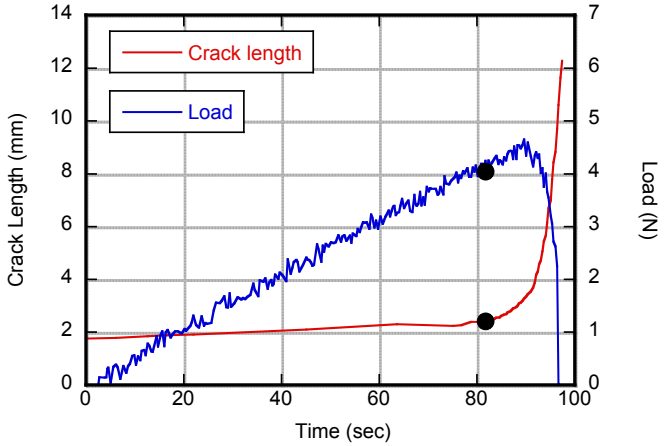

Figure 5. Crack Length and Load vs. Time for 20% Ballistic Gelatin at Low Rate

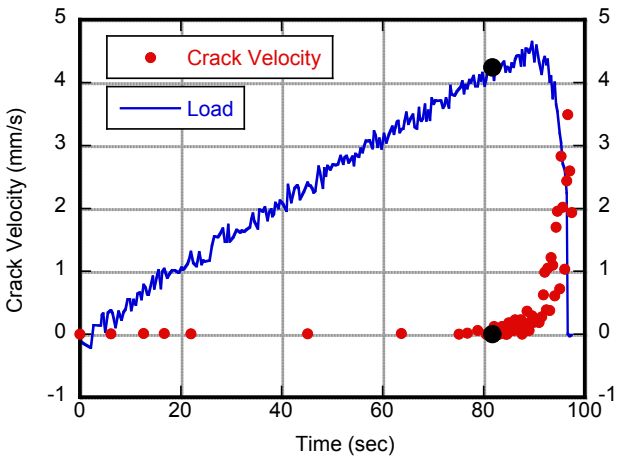

Figure 6. Crack Velocity and Load vs. Time for 20% Ballistic Gelatin at Low Rate

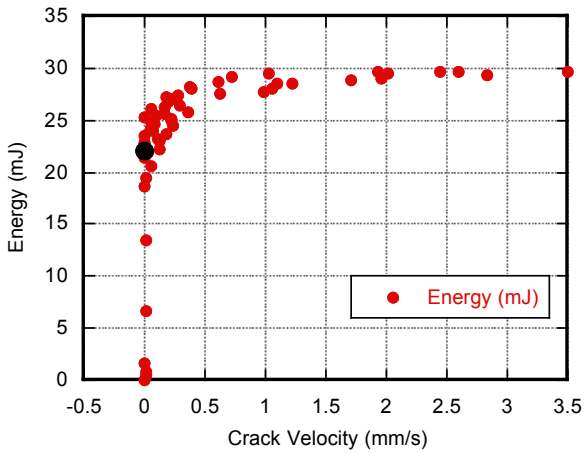

Figure 7. Energy vs. Crack Velocity for 20% Ballistic Gelatin at Low Rate

The preceding data is representative of the data obtained for 10% and 20% ballistic gelatin at low and high rates, and for Perma-Gel at low rate. Valid results for the Perma-Gel fracture experiments at 127 mm/s could not be obtained; the test machine reached its maximum extension (100 mm) prior to the crack propagating at this rate. The crack eventually would propagate to failure after being stretched to the maximum machine displacement and held there for a few seconds. In all cases, the fracture surfaces of the 10% and 20% ballistic gelatin as well as the Perma-Gel were very smooth and flat.

The complete data sets for all of the experiments that were conducted are not shown in this paper for brevity; the results are summarized in Table 1. There is a significant difference between the loading rates for 20% and 10% ballistic gelatins for identical displacement rates. At high rate, the average loading rate for 20% ballistic gelatin is about twice that of the 10%; the load at the initiation of crack growth is about 4 times higher in the 20% ballistic gelatin than the 10%. However, the load for initiation of crack growth for Perma-Gel at the low rate is lower than the 20% ballistic gelatin, yet the critical energy required for crack growth is higher. The total displacement to reach crack propagation for the Perma-Gel is higher than for both ballistic gelatins. In fact, the total displacement is about 40 mm for the Perma-Gel to reach complete specimen failure. For both ballistic gelatins, the corresponding extension is about 10-12 mm. The critical e_{yy} strain at the initiation of crack growth is ~0.20, approximately the same magnitude for the 10% and 20% ballistic gelatin; for the Perma-Gel it was 0.68, three times the value for the ballistic gelatins.

Table 1. Summary of Gelatin Fracture Experimental Results

Initial Crack Length (a) = 1.75 mm Width = 12.7 mm Thickness = 9.5 mm	10% Ballistic Gelatin		20% Ballistic Gelatin		Perma-Gel™	
Displacement Rate (mm/s)	0.127	127	0.127	127	0.127	127
Avg. Loading Rate (N/s)	0.00956	10.90	0.05020	20.86	0.00088	-
Load for Initiation of Crack Growth (N)	0.66	3.05	4.25	12.25	1.42	-
Critical Energy for Initiation of Crack Growth (mJ)	2.71	66.48	22.05	455.11	27.83	-
Critical e-yy for Initiation of Crack Growth	0.20	1.56	0.17	2.70	0.68	-

The energy imparted for both 10% and 20% ballistic gelatin as a function of the crack velocity at the displacement rate of 127 mm/s are shown in Figure 8(a). The black markers are the critical energy at crack initiation for each material. The critical energy for crack growth for the 10% and 20% ballistic gelatin is about 455 mJ and 67 mJ, respectively. For the Perma-Gel, at 127 mm/s, the crack growth never started; at maximum displacement, the energy level had already reached ~300 mJ. With about twice the amount of gelatin power by mass, the 20% ballistic gelatin is much more resilient to crack initiation than the 10% ballistic gelatin. After crack initiation, the crack would grow at a steady energy level for 10% ballistic gelatin. In contrast, the energy required for crack growth increases with crack velocity for 20% ballistic gelatin, after the start of crack growth. Figure 8(b) shows the energy as a function of crack velocity at the lower loading rate for both ballistic gelatins and the Perma-Gel.

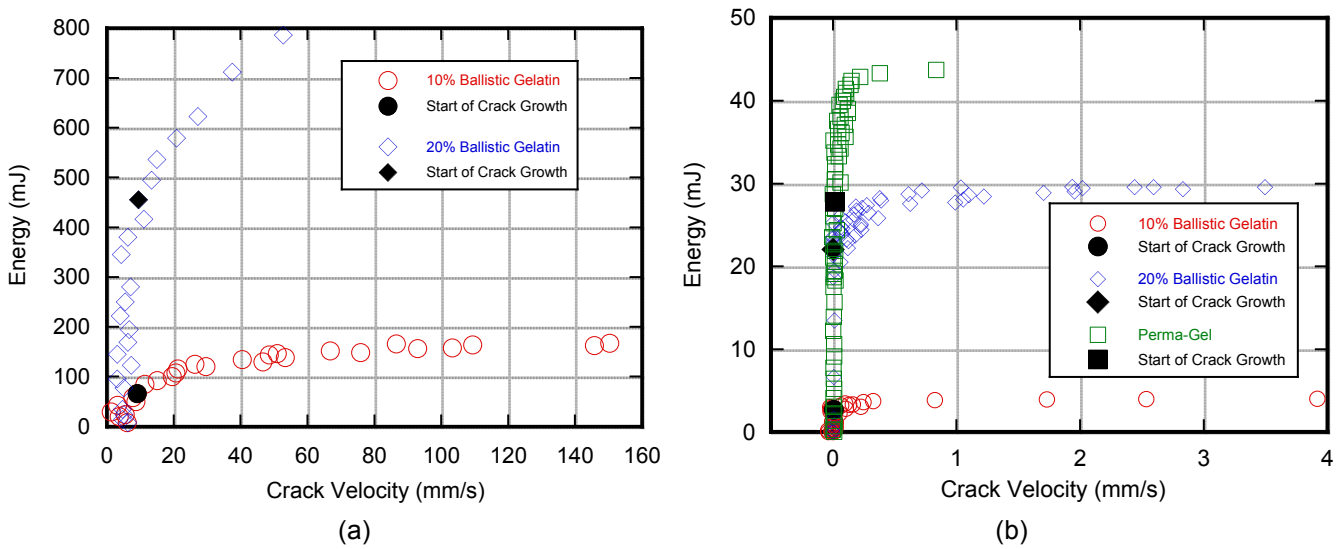

Figure 8. Energy as a Function of Crack Velocity for all Gelatins at (a) High Rate and (b) Slow Rate

The critical energy for Perma-Gel (27 mJ) is similar to the 20% ballistic gelatin at 22 mJ, and both are significantly greater than 10% ballistic gelatin (2.7 mJ). As can be seen in Figure 8(b), even after crack initiation in the Perma-Gel at low rate, the energy continues to increase until it reaches 43 mJ and levels off shortly before complete fracture. This continuation of increased energy absorption after crack initiation demonstrates just how much tougher the Perma-Gel is compared to the ballistic gelatins. This is also demonstrated by the fact that the Perma-Gel reached maximum displacement before crack initiation at the 127 mm/s rate. Also, at this loading rate, the critical energy required for crack growth for both gelatins decreases significantly in comparison with the high loading rate experiments.

All of the gelatins are much more resistance to crack initiation and propagation at higher rates. At the slower rate, there is more time for the crack to start during the experiment. The test time duration at the slower rate is about

90 seconds for the 10% and 20% gelatins whereas the Perma-Gel test ran for an average test time of 3 minutes to reach complete fracture. Furthermore, the time to reach the onset of the crack initiation in the Perma-Gel is much longer. The polymer gel is relatively tacky and this may have further increased its crack resistance. After notching, the crack in the Perma-Gel appears to seal itself.

Both at low and high rates, the energy required for crack initiation and growth for 10% and 20% ballistic gelatins are shown in Figures 9(a) and 9(b), respectively. Each plot also includes an expanded view of the low rate experiments. For both 10% and 20% ballistic gelatins, the energy required for crack initiation and growth is higher at the higher loading rate. Energy levels are higher for 20% gelatins compared to 10% gelatin for both initiation and growth of the crack for corresponding velocities of the crack. In both types of ballistic gelatins, at the slower loading rate, energy reached a steady value for further crack growth after initiation; however, for the higher loading rate, the energy did not reach a steady value during the crack growth.

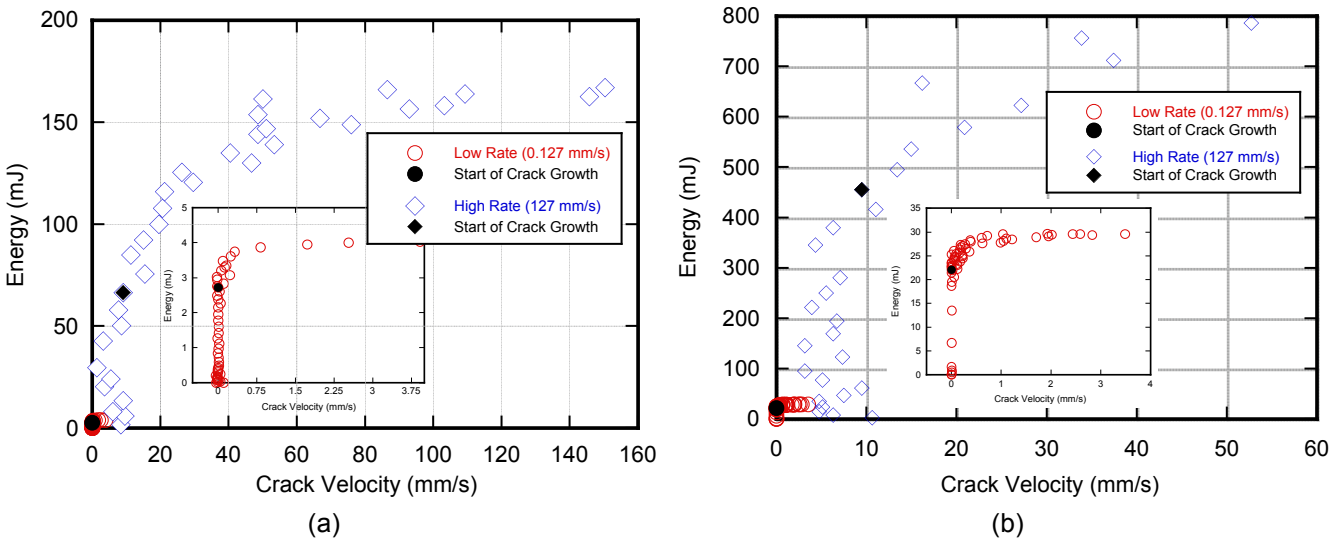

Figure 9. Energy as a Function of Crack Velocity at Low Rate and High Rate for (a) 10% Ballistic Gelatin and (b) 20% Ballistic Gelatin

SUMMARY AND CONCLUSIONS

Experimental methods were developed to obtain tensile failure criteria. These can be used for simulation of projectile penetration into different gels. Mode I fracture experiments, using single edge-notched specimens, were conducted at two different loading rates on three gelatins: 10% and 20% ballistic gelatin and polymer based Perma-Gel. Digital image correlation was used to measure the strain field at the crack tip during initiation and propagation. The critical energy for crack initiation and growth were determined from the experiments for all three gelatins at low loading rates; they were also determined for the two ballistic gelatins at high loading rate. Critical maximum strain in the loading direction for crack growth was obtained from the measured strain fields at the crack-tip. Results show a significant increase in the critical energy required for crack initiation and subsequent growth for both ballistic gelatins at the high rate compared to the slow rate. At the lower rate, Perma-Gel requires a higher critical energy for the crack initiation than both 10% and 20% ballistic gelatins. For the low loading rate, energy for further growth reached a steady value until complete failure; in contrast, for the high loading rate, the energy required for crack growth after initiation did not reach a steady value.

The critical maximum strain in the loading direction at the crack growth initiation was obtained for the gelatins at the tested loading rates. The critical maximum strain for crack growth initiation was an order of magnitude higher for the high loading rate, compared to the low rate. For Perma-Gel, the critical strain was about three times higher compared to that for ballistic gels at the slower rate of loading; comparatively, the critical strain for 10% and 20% ballistic gels were approximately at the same level for this loading rate. At the high loading rate, critical strain for the 20% gelatin was about two times higher. Results from these fracture experiments indicate that all the gelatins are rate sensitive and each gelatin behaves differently with respect to one another. These critical energy and strain-based criteria can be used as failure criteria during simulation of penetration into gels.

ACKNOWLEDGEMENTS

The authors wish to acknowledge the following individuals at the U.S. Army Research Laboratory for providing the Perma-Gel material and information on the procedure to fabricate these materials: Mr. Larry Long and Mr Richard Merrill.

Certain commercial equipment and materials are identified in this paper in order to specify adequately to the experimental procedure. In no case does such identification imply recommendation by the Army Research Laboratory nor does it imply that the material or equipment identified is necessarily the best available for this purpose.

REFERENCES

1. Peterson, B. Ballistic Gelatin Lethality Performance of 0.375-in Ball Bearings and MAAWS 401B Flechettes. Army Research Laboratory Technical Report. ARL-TR-4153. 2007
2. Nicolas, N. C. and Welsch, J. R. Ballistic Gelatin, Institute for Non-Lethal Defense Technologies Report, The Pennsylvania State University Applied Research Laboratory.
3. MacPherson, D. Bullet Penetration: Modeling the Dynamics and the Incapacitation Resulting from Wound Trauma. Ballistic Publications. 1994.
4. Fackler, M. L. Ordnance Gelatin for Ballistic Studies. Association of Firearm and Toolmark Examiners Journal. 4:403-5. 1987.
5. http://en.wikipedia.org/wiki/ballistic_gelatin
6. Moy, P., Weerasooriya, T., Juliano, T.F., VanLandingham, M.R., and Chen, W. Dynamic Response of an Alternative Tissue Simulant, Physically Associating Gels (PAG). Proceedings of the 2006 SEM Annual Conference. St. Louis, MO. 2006.
7. Salisbury, C.P. and Cronin, D.S., Mechanical Properties of Ballistic Gelatin at High Deformation Rates, Experimental Mechanics. 2009.
8. Juliano, T.F., Forster, A. M., Drzal, P.L., Weerasooriya, T., Moy, P., and VanLandingham, M.R., Multiscale Mechanical Characterization of Biomimetic Physically Associating Gels. J. Mater. Res., Vol 21, No. 8, Aug 2006.
9. Moy, P., Weerasooriya, T., and Gunnarsson, C. A., Tensile Deformation of Ballistic Gelatin as a Function of Loading Rate. Proceedings of the 2008 SEM Annual Conference. Orlando, FL. 2008.
10. Zhang, H. P., Niemczura, J., Dennis, G., Ravi-Chandar, K., and Marder, M. Toughening Effect of Strain-Induced Crystallites in Natural Rubber. Physical Review Letters, Vol. 102, Issue 24, id. 245503. June 2009.
11. Moy, P., Weerasooriya, T., and Gunnarsson, C. A., Tensile Deformation and Fracture of Ballistic Gelatin as a Function of Loading Rate. Proceedings of the 2009 SEM Annual Conference. Albuquerque, NM. June 2009.
12. Chu, T. C., Ranson, W. F., Sutton, M. A., and Peters, W. H. Applications of Digital-Image-Correlation Techniques to Experimental Mechanics. Experimental Mechanics. September 1995.
13. Sutton, M. A., Wolters, W. J., Peters, W. H., Ranson, W. F., and McNeill, S. R. Determination of Displacements Using an Improved Digital Image Correlation Method. Computer Vision. August 1983.
14. Bruck, H. A., McNeill, S. R., Russell S. S., Sutton, M. A. Use of Digital Image Correlation for Determination of Displacements and Strains. Non-Destructive Evaluation for Aerospace Requirements. 1989.
15. Sutton, M. A., McNeill, S. R., Helm, J. D., Schreier, H. Full-Field Non-Contacting Measurement of Surface Deformation on Planar or Curved Surfaces Using Advanced Vision Systems. Proceedings of the International Conference on Advanced Technology in Experimental Mechanics. July 1999.
16. Sutton, M. A., McNeill, S. R., Helm, and Chao, Y. J. Advances in Two-Dimensional and Three-Dimensional Computer Vision. Photomechanics. Volume 77. 2000.